MIM and Cortactin Antagonism Regulates Ciliogenesis and Hedgehog Signaling

Marina Bershteyn,[1,2] Scott X. Atwood,[1] Wei-Meng Woo,[1] Mischa Li,[1] and Anthony E. Oro[1,*]
[1]Program in Epithelial Biology
[2]Cancer Biology Graduate Program
Stanford University, School of Medicine CCSR 2145c, 269 Campus Drive, Stanford, CA 94305, USA
*Correspondence: oro@stanford.edu
DOI 10.1016/j.devcel.2010.07.009

SUMMARY

The primary cilium is critical for transducing Sonic hedgehog (Shh) signaling, but the mechanisms of its transient assembly are poorly understood. Previously we showed that the actin regulatory protein Missing-in-Metastasis (MIM) regulates Shh signaling, but the nature of MIM's role was unknown. Here we show that MIM is required at the basal body of mesenchymal cells for cilia maintenance, Shh responsiveness, and de novo hair follicle formation. MIM knockdown results in increased Src kinase activity and subsequent hyperphosphorylation of the actin regulator Cortactin. Importantly, inhibition of Src or depletion of Cortactin compensates for the cilia defect in MIM knockdown cells, whereas overexpression of Src or phospho-mimetic Cortactin is sufficient to inhibit ciliogenesis. Our results suggest that MIM promotes ciliogenesis by antagonizing Src-dependent phosphorylation of Cortactin and describe a mechanism linking regulation of the actin cytoskeleton with ciliogenesis and Shh signaling during tissue regeneration.

INTRODUCTION

Primary cilia are solitary microtubule-based organelles that protrude from the cell surface and function in transducing extracellular signals (Davenport and Yoder, 2005). Defects in cilia structure or associated signaling proteins alter sensitivity to mechanical and developmental cues and result in a diverse array of developmental abnormalities (renal cysts, respiratory and visual disorders, a predisposition to obesity, diabetes, and hypertension) that are seen in diseases with dysfunctional cilia, collectively termed "ciliopathies" (Adams et al., 2008; Fliegauf et al., 2007).

Cilia assemble transiently during cell cycle quiescence or G1-phase followed by programmed disassembly prior to mitosis (Dawe et al., 2007; Marshall, 2008; Pearson et al., 2007). The mother centriole, characterized by distal and subdistal appendages such as Cenexin1, Ninein, and Cep164 (Lange and Gull, 1995; Mogensen et al., 2000; Graser et al., 2007), functions as a basal body at the plasma membrane to provide a template for ciliary microtubules and a docking station for intraflagellar transport (IFT) machinery during primary cilia elongation. Cilium membrane growth requires localized recruitment and activation of Rab8, which is mediated by the conserved complex of BBS proteins and Rabin8 GEF activity (Nachury et al., 2007). Although many of the structural components required for primary cilia formation have been identified, the mechanisms that coordinate the timing of cilia assembly and disassembly with the cell cycle are still largely unknown.

Improperly formed or absent primary cilia impair cells' ability to respond to the morphogen Shh (Huangfu and Anderson, 2005). The Shh pathway regulates organ patterning and tissue homeostasis and is implicated in many genetic disorders and malignancies (Chari and McDonnell, 2007). Mice with mutations in genes encoding for ciliary structural components such as Ift88 or Kif3a have developmental defects in the limbs, neural tube, and hair follicles that are characteristic of aberrant Shh signaling (Caspary et al., 2007; Huangfu et al., 2003; Lehman et al., 2009). The list of proteins that affect both Shh signaling and cilia formation has been growing, but the biochemical functions of these proteins have not been precisely elaborated in most cases (Houde et al., 2006; Norman et al., 2009; Ruiz-Perez et al., 2007).

The hair follicle constitutes a valuable, genetically tractable model system of organ development and regeneration as it undergoes periodic cycles of self-renewal through reciprocal signaling between epithelia-derived keratinocytes and mesenchyme-derived dermal papilla cells (Schneider et al., 2009). During hair follicle morphogenesis, Shh is expressed in epithelial placodes and stimulates keratinocyte proliferation and dermal papilla maturation (Chiang et al., 1999; Karlsson et al., 1999; St-Jacques et al., 1998). Recent studies demonstrated that conditional deletion of *Ift88* or *Kif3a* in ventral dermis resulted in a severely reduced number of hair follicles that were arrested at stage 2 of morphogenesis (Lehman et al., 2009), phenocopying loss of Shh signaling in skin (Chiang et al., 1999; St-Jacques et al., 1998). These results revealed a central role of the dermal primary cilia in hair follicle development and underscored the need to understand the mechanisms of cilia regulation during tissue regeneration and cycling.

In a screen for hedgehog target genes, we previously identified Missing-in-Metastasis (MIM), a Bin/Amphiphysin/Rvs (BAR) domain containing protein of the IRSp53-MIM-Domain (IMD) family (Machesky and Johnston, 2007). MIM is able to bind to the intracellular mediators of Shh signaling Sufu and Gli and positively regulate the pathway (Callahan et al., 2004). Additional gain-of-function studies showed that MIM regulates actin

cytoskeleton dynamics and interacts with Cortactin (CTTN), a key substrate of the oncogenic Src kinase and a major activator of actin branching and polymerization (Bompard et al., 2005; Gon-zalez-Quevedo et al., 2005; Lin et al., 2005; Mattila et al., 2003; Yamagishi et al., 2004b). However, a demonstration of endogenous MIM function has been lacking. Here we used loss-of-function methods to show that MIM is part of a basal body complex required for primary cilia maintenance and Shh signaling, and functions by a mechanism that involves antagonism of CTTN phosphorylation by p60 Src kinase. In addition, we show that MIM is required in the dermal papilla for primary cilia formation and hair follicle regeneration. Our data link MIM with an actin regulatory pathway controlling ciliogenesis and Shh signaling.

RESULTS

MIM Is Required for Primary Cilia Formation

We used short hairpins expressed from a lentiviral vector (Ventura et al., 2004) to deplete *MIM* mRNA in several cell types of mesenchymal origin including primary dermal cells from newborn mouse skin, 10T1/2 cells and MEFs. In each case, we observed a striking decrease in primary cilia that correlated with the efficiency of *MIM* knockdown (hereafter referred to as MIM KD) using three independent hairpins (Figures 1A–1D and S1, available online). Since cilia form during G1/G0, we used FACS analysis to confirm that MIM KD in cells cultured under the conditions that promote cilia formation does not affect cell cycle distribution (Figures S1A–S1C). In addition, we confirmed that MIM KD does not alter cell proliferation or apoptosis (Figures S1D–S1G). Thus, the decrease in primary cilia with reduction in MIM levels is not attributable to cell cycle differences and points to a direct role for MIM in either primary cilia formation or maintenance.

To further characterize the ciliary defect in MIM KD cells, we analyzed the status of several shaft, basal body, and centriolar proteins. Staining with antibodies to ciliary shaft components such as acetylated α-tubulin, IFT88, and glutamylated tubulin indicated that the structure does not form in MIM KD cells (Figures 1E and 1J; data not shown). Despite the apparent lack of ciliary shaft, the basal body was detected by pericentrin staining (Figure 1E). Centriole duplication was confirmed by staining with antibody to γ-tubulin (Figure 1F, green dots). Finally, basal body maturation also appears normal in MIM KD cells as assessed by expression of distal and subdistal appendage proteins preferentially localized at the mother centriole such as Cenexin1, Ninein, and Cep164 (Figures 1G–1I) (Lange and Gull, 1995; Mogensen et al., 2000; Graser et al., 2007). These studies suggest that MIM is required for forming or maintaining the ciliary shaft and not for centriole duplication or maturation.

Endogenous MIM Is Enriched at and Associates with the Centrosome/Basal Body

Next, we analyzed localization of endogenous MIM and found that in wild-type primary dermal cells, 10T1/2, or MEFs MIM immunoreactivity is enriched at the basal body and to a lesser degree can be found at the plasma membrane and in cytoplasmic/nuclear puncta (Figures 2A, 2C, S2A, and S2B; data not shown). The immunoreactivity at the basal body colocalizes with γ-tubulin and is specific to MIM, as staining disappears in MIM KD cells (Figures 2A–2D). MIM localization at the centro-

somes persists throughout the cell cycle, in mitotic and interphase cells with or without a primary cilium (Figures S2A and S2B). Moreover, in cells that still have cilia following MIM KD, MIM expression is detected at the basal body (Figures S2A and S2B), suggesting that some primary cilia remain due to incomplete knockdown.

To confirm MIM association with the centrosome, we biochemically isolated centrosomes from 10T1/2 cells (Meigs and Kaplan, 2008) and analyzed sucrose fractions from the final purification step by western blot. Similar to other centrosomal proteins that were identified using this method (Kaplan et al., 2004), MIM cofractionates with γ-tubulin (Figure 2E). The band at ∼102 kDa is detected by antibodies raised against both N- and C-terminal portions of MIM (Figure 2E; data not shown), indicating that full-length MIM is at the centrosome. Moreover, immunoprecipitation of endogenous MIM from dermal cell lysates coimmunoprecipitates γ-tubulin (Figure 2F). Taken together, these data indicate that MIM is a centrosome-associated protein that regulates ciliogenesis.

MIM Localizes to the Basal Body and Rescues Cilia Independent of the BAR Domain

To determine which portions of MIM regulate basal body localization, we expressed different truncations of human MIM (hMIM) tagged with GFP. GFP alone is mostly nuclear and does not localize to the basal body (Figure 2G). The N terminus of MIM contains a conserved BAR domain known to localize to the plasma membrane and to induce membrane protrusions (Gonzalez-Quevedo et al., 2005; Lin et al., 2005; Mattila et al., 2007; Yamagishi et al., 2004b). Consistently, the N-terminal BAR domain-containing construct of hMIM (hMIM 1-277) is predominantly cytoplasmic and membrane-associated and does not localize to the basal body (Figure 2H). By contrast, two C-terminal constructs lacking the BAR domain (hMIM 277-755 and 400-755) are cytoplasmic with strong enrichment at the basal body (Figures 2I and 2J).

Next, we asked which portions of MIM can rescue cilia by transfecting GFP-tagged hMIM constructs in the presence of mouse MIM KD and analyzing primary cilia in GFP-positive cells. We found that hMIM 1-277, which does not localize to the basal body (Figure 2H), does not rescue cilia after MIM KD (Figure 2K). On the other hand, hMIM 277-755 and 400-755, both of which localize to the basal body, significantly rescue primary cilia (Figure 2K). These data suggest that MIM's localization to the basal body is independent of the BAR domain and potentially implicate C-terminal binding partners in MIM-dependent cilia regulation.

Actin Polymerization Inhibits Cilia Elongation and Promotes Cilia Disassembly

One of the best characterized C-terminal binding partners of MIM is a regulator of actin branching and polymerization Cortactin (CTTN) (Lin et al., 2005). Since MIM was shown to inhibit CTTN-mediated actin polymerization in vitro (Lin et al., 2005), we decided to investigate the role of actin and CTTN in ciliogenesis. We treated serum-starved 10T1/2 and primary dermal cells with actin depolymerizing drugs cytochalasin D or B for 90 min and examined the effect on primary cilia. Surprisingly, disruption of F-actin with either agent results in significantly longer cilia
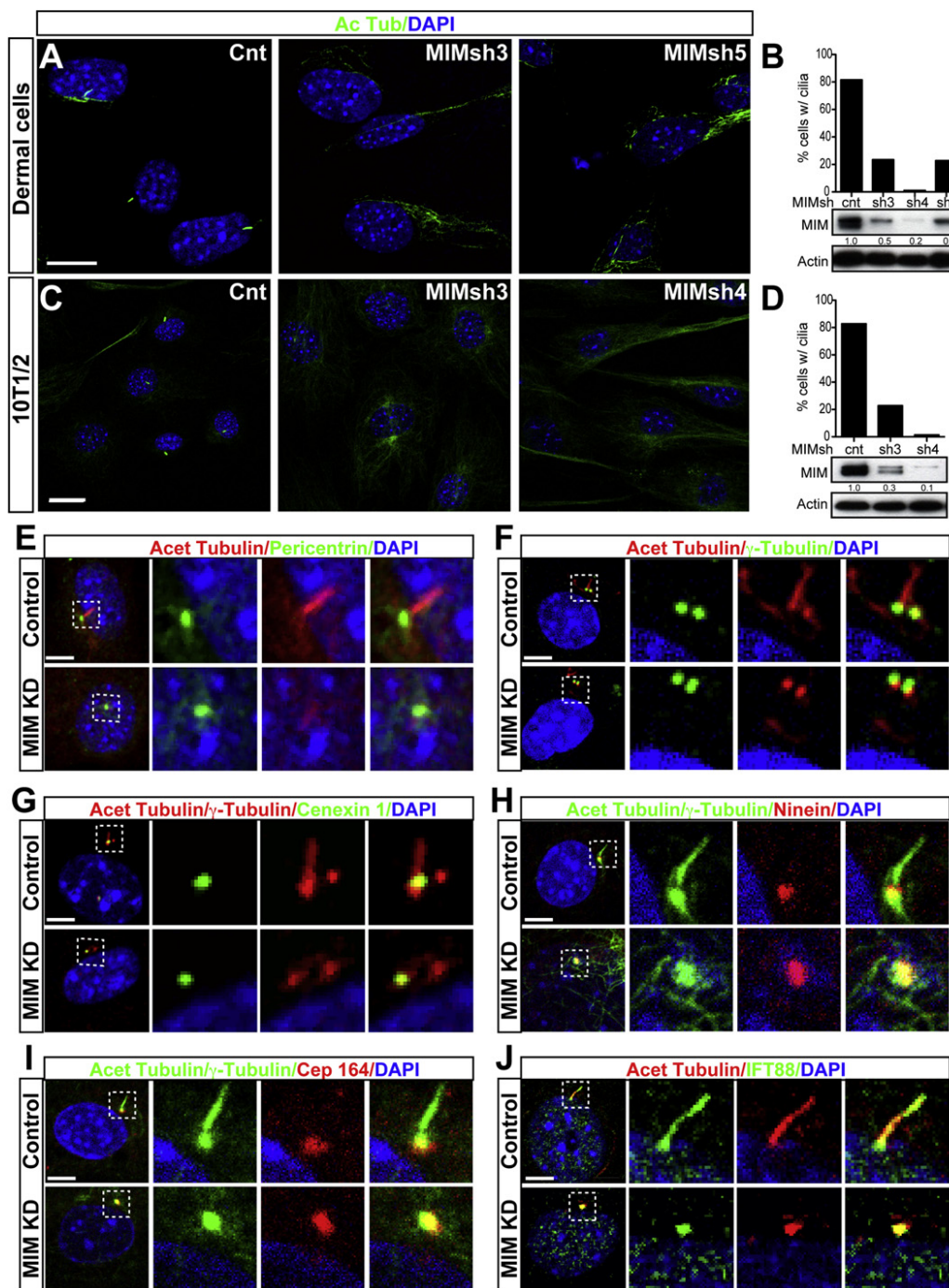
**Figure 1. MIM Is Required for Primary Cilia Formation**

(A–D) Primary dermal cells from mouse skin (A and B) and 10T1/2 cells (C and D) were serum starved overnight and stained for primary cilia with antibody to acetylated α-tubulin (green) and DNA (blue). Representative fields are shown in (A) and (C). Scale bar is 10 μm. (B and D) Percentage of cells with primary cilia in dermal (B) and 10T1/2 (D) cells following MIM KD. More than 300 cells from representative fields were analyzed. Below each graph is a corresponding Western analysis for MIM and Actin. The numbers below the MIM blots indicate relative MIM protein levels in each lane based on densitometry measurements performed with ImageJ software.

(E–J) IF of representative control or MIM KD primary dermal cells with indicated antibodies to basal body, centrioles, and ciliary shaft proteins. Scale bar represents 5 μm. Regions within the boxes outlined by a dotted white line are shown at higher magnification to the right.

(Figures 3A, 3B, and 3D)—a response that is partially reversible after the drug is washed away (Figure 3C). Since actin polymerization inhibits cilia elongation, we asked whether it also promotes cilia disassembly. Addition of serum-containing media with DMSO to contact inhibited serum-starved cells significantly reduces average cilia length within 4 hr (Figures 3D–3F),
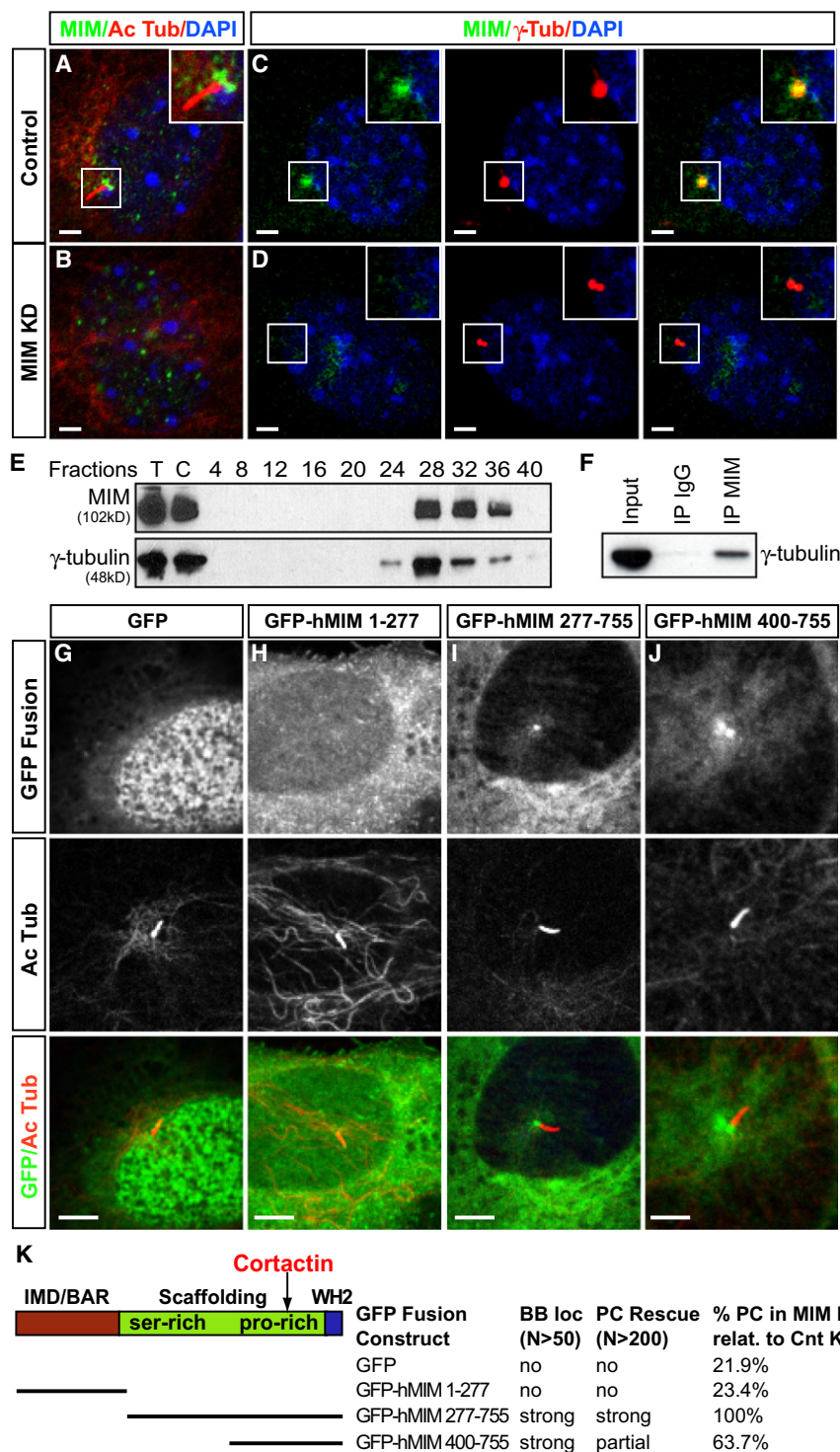
Figure 2. MIM Localizes to the Basal Body

(A–D) IF of representative control (A and C) and MIM KD (B and D) dermal cells with antibodies to MIM (green), acetylated α-tubulin (A and B, red) or γ-tubulin (C and D, red) and DNA (blue). Scale bar represents 2 μm. Regions inside the white boxes are shown at higher magnification in the top right corner of the corresponding panels.

(E) Western analysis for MIM and the centrosomal marker γ-tubulin after isolation of centrosomes from 10T1/2 cells. T = total cell lysate; C = crude extract prior to sucrose fractionation.

(F) Western analysis for γ-tubulin after immunoprecipitation (IP) with control IgG or antibody against MIM from primary dermal cell lysates.

(G–J) Cells were transfected with various GFP-hMIM constructs and stained with antibody to acetylated α-tubulin (red). Scale bar represents 5 μm.

(K) Schematic of MIM structural domains (with an arrow pointing out the proline-rich region in the C terminus of MIM that interacts with Cortactin) and the GFP-hMIM constructs used in this study. On the right side is a summary of basal body localization and cilia rescue activity in primary mouse dermal cells based on three separate experiments. The last column shows percentage of GFP-positive MIM KD cells with primary cilia normalized to GFP-positive control (Cnt) cells.

GFP Fusion Construct	BB loc (N>50)	PC Rescue (N>200)	% PC in MIM KD relat. to Cnt KD
GFP	no	no	21.9%
GFP-hMIM 1-277	no	no	23.4%
GFP-hMIM 277-755	strong	strong	100%
GFP-hMIM 400-755	strong	partial	63.7%

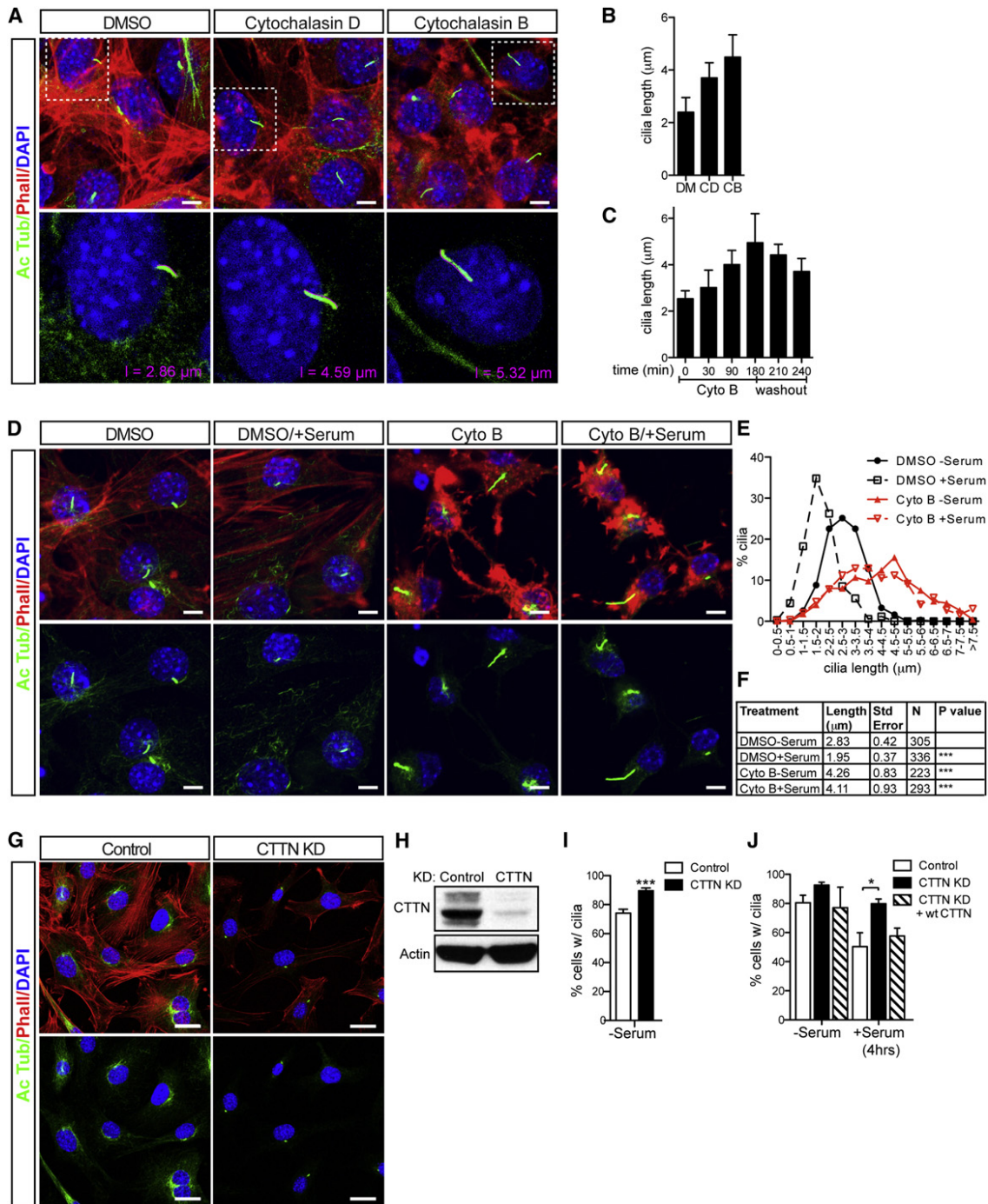## Cortactin Inhibits Ciliogenesis and Promotes Cilia Disassembly

Next, we examined the role of CTTN in ciliogenesis. CTTN KD in primary mouse dermal cells yields the expected decrease in F-actin structures (Figure 3G) and a modest but consistent increase in percentage of ciliated cells, which can be rescued by putting wild-type rat CTTN back into cells (Figures 3H–3J). Interestingly, while initial cilia formation assessed 4 hr after plating cells is not affected by CTTN KD (Figure S3A), cilia disassembly is delayed, with more and longer cilia observed at every time point after addition of serum (Figures 3J, S3A, and S3B). Thus, CTTN has the opposite effect from MIM and appears to inhibit primary cilia formation and/or promote disassembly.

MIM Regulates Cilia Formation by Antagonizing Cortactin

The intriguing opposition of MIM and CTTN phenotypes prompted us to investigate the biochemical and functional interaction between the two proteins during ciliogenesis. We detected low levels of CTTN-specific immunoreactivity at and around the basal body (Figures S3C) and found that γ-tubulin coimmunoprecipitates with CTTN from cell lysates, although the interaction appears to be more robust during G2/M (Figure S3D). Our results are consistent with a recent finding that phosphorylated CTTN is

indicating cilia disassembly. By contrast, the same experiment done in the presence of cytochalasin B results in a much broader cilia length distribution and a failure of cilia disassembly (Figures 3D–3F). In addition, the fact that upon inhibition of actin polymerization the two curves with and without serum overlap (Figure 3E) suggests that actin mediates the effect(s) of serum on cilia disassembly.

Figure 3. Actin and Cortactin Inhibit Ciliogenesis

(A, D, and G) IF with antibody to acetylated α-tubulin (green), phalloidin (red), and DNA (blue). (A and B) Serum-starved 10T1/2 cells were treated for 90 min with DMSO, cytochalasin D, or cytochalasin B prior to fixation and staining. (A) Representative images. Scale bar represents 5 μm. Regions within white dotted boxes are shown at higher magnification in the bottom panels. Cilia in the bottom panels were measured using LSM image browser software, and the lengths are shown in the lower right corner. (B) Corresponding average cilia lengths. DM = DMSO; CD/CB = cytochalasin D or B, respectively. At least 40 cilia were measured from each treatment group. Error bars show SD. (C) Average primary cilia lengths in 10T1/2 cells treated with cytochalasin B followed by drug washout for the indicated time periods. At least 30 cilia were measured from each time point. Error bars show SD. (D–F) Confluent primary dermal cells were serum starved overnight and then incubated with serum-free or 10% FBS containing medium supplemented with DMSO or cytochalasin B for 4 hr prior to fixation and staining. (D) Representative images. Scale bar represents 5 μm. (E) Cilia lengths distribution. Over 200 cilia were measured from each treatment group in three separate experiments. (F) Summary of the results. The difference between cilia lengths in cytochalasin B-treated cells ± serum is not statistically significant. (G–I) Following control or cortactin knockdown (KD) in primary dermal cells, equal numbers of cells were plated and serum starved overnight prior to fixation and staining. (G) Representative images. Scale bar represents 10 μm. (H) Western analysis for CTTN and Actin following CTTN KD. (I) Percentage of cells with primary cilia. More than 1500 cells were analyzed from each treatment group in six separate experiments. Error bars show SEM. (J) Primary mouse dermal cells from control,
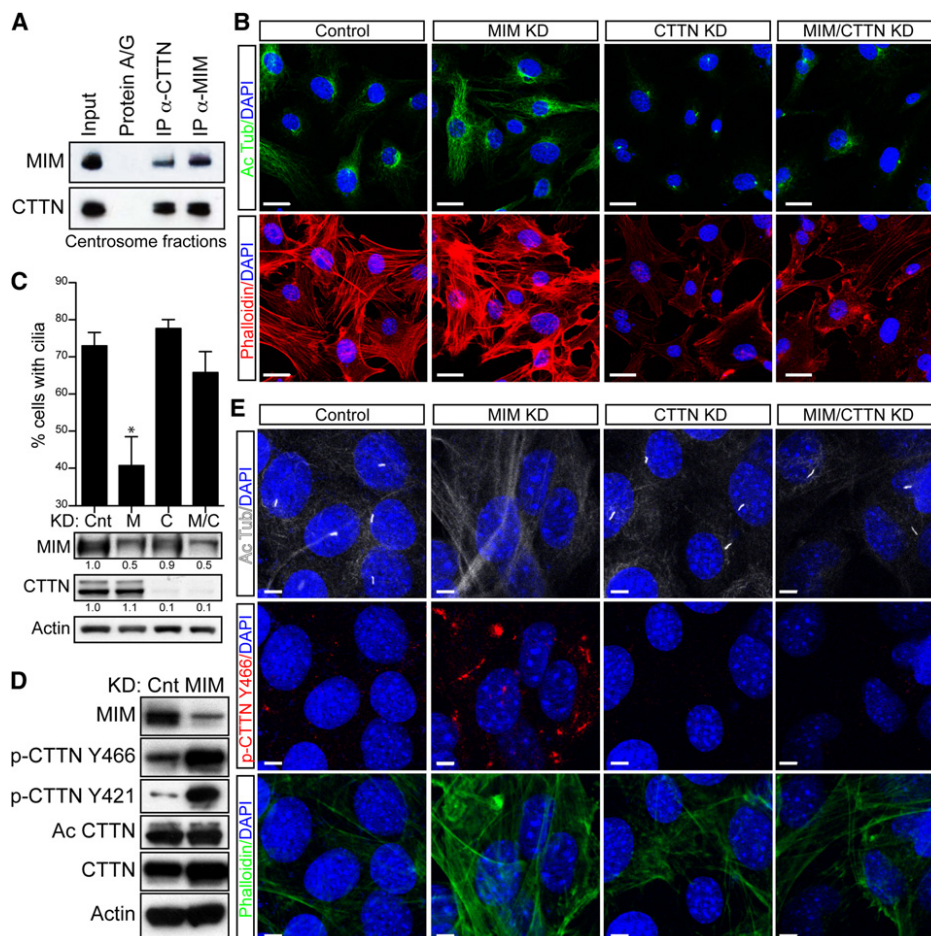
Figure 4. MIM Promotes Ciliogenesis by Antagonizing Cortactin

(A) Western analysis for MIM and CTTN after immunoprecipitation with antibodies to MIM or CTTN from γ-tubulin-positive centrosomal fractions isolated from 10T1/2 cells.

(B and C) Following control, MIM, CTTN, or MIM/CTTN KD, equal numbers of confluent primary dermal cells were serum starved overnight. (B) Representative IF with antibody to acetylated α-tubulin (green), phalloidin (red), and DNA (blue). Scale bar represents 20 μm. (C) Percentage of cells with cilia with corresponding western blots for MIM, CTTN, and Actin. More than 850 cells were analyzed from each knockdown group in three separate experiments. Error bars show SEM. *p < 0.05. There is no statistically significant difference between MIM/CTTN KD and control.

(D) Western analysis for the indicated proteins in serum-starved dermal cell lysates after control or MIM KD.

(E) The experiment described in (B) and (C) was performed in 10T1/2 cells. Representative images of IF with antibodies to acetylated α-tubulin (white), pCTTN-Y466 (red), phalloidin (green), and DNA (blue). Scale bar represents 5 μm.

enriched at the centrosomes during G2/M where it interacts with γ-tubulin (Wang et al., 2008; Figure S3E). Furthermore, endogenous MIM and CTTN mutually coimmunoprecipitate from γ-tubulin-positive centrosome fractions (Figure 4A), supporting that MIM and CTTN complexes are associated with the centrosomes.

Given the opposing roles of MIM and CTTN in ciliogenesis we examined their functional interaction by concomitant depletion of both proteins. Surprisingly, simultaneous KD of MIM and CTTN in dermal or 10T1/2 cells significantly restores primary cilia

(Figures 4B, 4C, and 4E, top row), suggesting that MIM antagonizes CTTN to promote ciliogenesis. To understand the molecular basis of this antagonism, we looked for possible alterations in the levels of CTTN posttranslational modifications after MIM KD. Analysis of G1 cells following MIM KD revealed a modest increase in total CTTN levels and a marked increase in phosphorylated CTTN at tyrosine residues 466 and 421 (Figures 4D and 4E, middle row). This phenotype is specific to MIM KD as it is seen with multiple hairpins (Figure S5A; data not shown). The increase in p-CTTN levels in MIM KD cells correlates with

CTTN KD or CTTN KD transfected with wt human CTTN were serum starved for 24 hr. During the final 4 hr prior to fixation and staining, half of the cells were incubated with medium containing 10% FBS. Percentage of cells with primary cilia. For control and CTTN KD, more than 1200 cells were analyzed from each treatment group in four separate experiments. For the rescue experiment, more than 225 transfected cells were analyzed in two separate experiments. Error bars show SEM. Statistics: unpaired two-tailed t tests were done for experiments that were performed at least three times. Stars indicate statistically significant differences. *p < 0.05; **p < 0.01; ***p < 0.001.
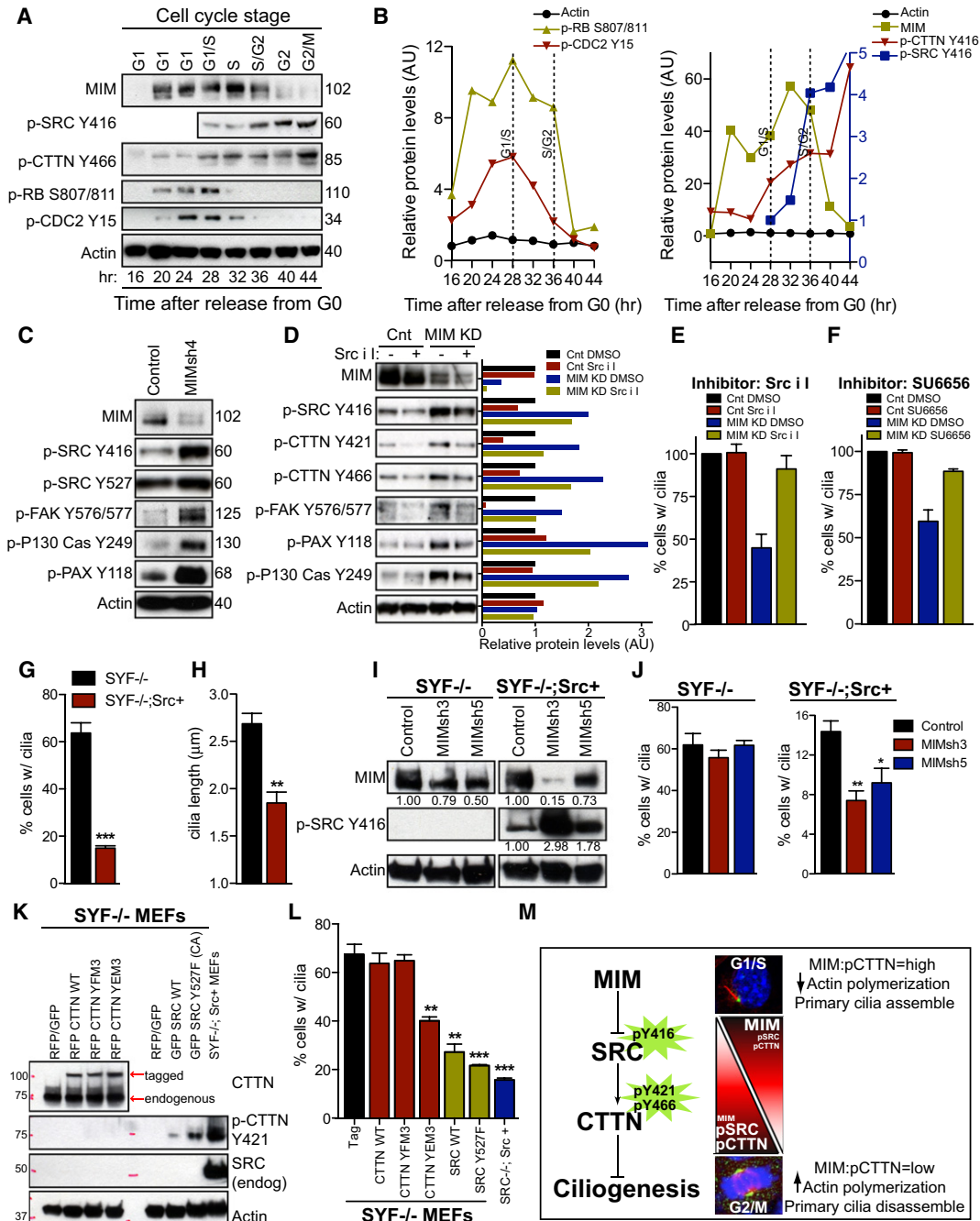
Figure 5. MIM Promotes Ciliogenesis by Inhibiting Src Kinase Activation

(A) Western analysis for the indicated proteins during cell cycle progression of primary dermal cells synchronized by serum starvation (see Experimental Procedures). Densitometry was performed with ImageJ software.

(B) Expression of cell cycle proteins p-RB S807/811 and p-CDC2 Y15 was used to determine the timing of G1/S transition (left graph). MIM levels are higher in G1/S and decrease during G2/M, whereas p-Src Y416 and p-CTTN Y466 levels progressively increase toward G2/M (right graph). Note: there was not enough sample from the earlier time points to analyze p-Src, which is why relative p-Src protein levels were normalized against the 28 hr sample and plotted against the right y axis.

(C) Western analysis for MIM, p-Src, and several indicated Src substrates in serum-starved dermal cell lysates after control or MIM KD.

(D–F) Serum-starved control and MIM KD dermal cells were treated with Src inhibitor I for 2 hr (D and E) or SU6656 for 6 hr (F). (D) Western analysis with relative protein levels represented by the bar graph. Note that hyperphosphorylation of SRC substrates in MIM KD cells is at least partially reversible upon Src inhibition for just 2 hr. (E and F) Percentage of cells with cilia normalized to control DMSO samples. More than 400 cells were analyzed from each treatment group in two separate experiments.

(G and H) Cilia analysis in confluent serum-starved *SYF*^{−/−} and *SYF*^{−/−}*; Src*+ MEFs. (G) Percentage of cilia. More than 750 cells were analyzed in four experiments. (H) Cilia length. More than 150 cilia were measured.

increased F-actin staining (Figures 4B and 4E, bottom row). To the contrary, the level of acetylated CTTN is unaffected in MIM KD cells (Figure 4D).

Notably, CTTN was shown to be a substrate of the tubulin deacetylase HDAC6 (Zhang et al., 2007), and the defect in cilia resorption that we observed upon CTTN KD was reminiscent of the phenotype seen upon inhibition or knockdown of HDAC6 in retinal pigmented epithelial cells (Pugacheva et al., 2007). However, another study found that HDAC6 mutant mice were viable and had normal cilia (Zhang et al., 2008), prompting us to ask whether inhibition of HDAC6 could prevent cilia disassembly in MIM KD cells. We treated cells with an HDAC6-specific inhibitor Tubacin (Haggarty et al., 2003) or the general deacetylase inhibitor TSA (Yoshida et al., 1990) and found that, while both of these drugs cause a robust increase in the acetylation of microtubules, they do not alter the levels of acetylated CTTN nor do they compensate for reduced cilia in MIM KD cells (Figures S4A–S4C). Moreover, we also tested the effect of Aurora A kinase, shown to regulate cilia disassembly upstream of HDAC6 (Pugacheva et al., 2007) and similarly found that inhibition of the Aurora family of kinases is not sufficient to restore primary cilia in MIM KD cells (Figures S4B and S4C). Similar results are seen using shRNAs against HDAC6 and Aurora A kinase in conjunction with MIM KD (data not shown), suggesting that the AuroraA/HDAC6 pathway is distinct from the MIM/CTTN pathway during cilia disassembly.

MIM Inhibits Src Kinase Activation

The antagonistic relationship between MIM and CTTN led us to hypothesize that increased levels of phospho-CTTN underlie the cilia defect seen in MIM KD cells. CTTN phosphorylation at tyrosine resides 466 and 421 is mediated by the Src family of nonreceptor tyrosine kinases (SFKs) (Ammer and Weed, 2008). Interestingly, we found that the relative levels of MIM negatively correlate with p-CTTN Y466 and the activated p-Src Y416 over the cell cycle (Figures 5A and 5B), with MIM being enriched during G1/S (cilia formation/maintenance) and p-CTTN Y466/p-Src Y416 being enriched during G2/M (cilia disassembly/centrosomal separation).

One explanation of the striking increase in p-CTTN Y466/Y421 levels detected in MIM KD cells during G1 could therefore be increased activity of the p60 Src kinase. Indeed, upon MIM KD with three different hairpins we found increased levels of the activating p-Src Y416 associated with cytoplasmic puncta and the basal body, and no change in the levels of the autoinhibitory

p-Src Y527 (Figures 5C, S5A, and S5B). In addition, multiple actin-associated SRC substrates besides CTTN, including focal adhesion kinase (FAK), paxillin (PAX), and P130/Cas, are hyperphosphorylated in MIM KD cells (Figures 5C and S5A). These data suggest that MIM-dependent antagonism of CTTN is mediated by the Src family of tyrosine kinases and implicate p60 Src in cilia regulation.

Increased Src Activity Inhibits Ciliogenesis Downstream of MIM

The ectopic Src activity and increased p-CTTN levels seen in MIM KD cells led us to test whether inhibition of the Src catalytic domain could restore ciliary elongation. Using several small molecules targeting the Src family of tyrosine kinases (SFKs), we found that inhibition of Src activity partially or completely reverses both hyperphosphorylation of substrates and cilia reduction in MIM KD cells without affecting cilia in control cells (Figures 5D–5F and S5C, and data not shown). To rule out off-target effects of the small molecule inhibitors, we obtained fibroblasts from *Src/Yes/Fyn* triple knockout mouse embryos ($SYF^{-/-}$ MEFs) as well as the same MEFs overexpressing p60 *Src* ($SYF^{-/-}$; *Src+* MEFs). Strikingly, comparison of $SYF^{-/-}$ versus $SYF^{-/-}$; *Src+* MEFs revealed that the latter have very few and significantly shorter primary cilia (Figures 5G, 5H, and S5D), despite retaining the ability to stay in G1/G0 when grown under the conditions that promote ciliogenesis (Figures S5E and S5F). Moreover, we tested the effect of Src activity in dermal cells by infecting them with retroviral constructs expressing either kinase dead (K295R) or constitutively active (Y527F) Src followed by selection for positive clones. We found that Src K295R functions as a dominant-negative with respect to p-CTTN Y466 and promotes significantly higher numbers of cells with longer primary cilia (Figures S5G and S5H). On the other hand, Src Y527F strongly induces CTTN phosphorylation and results in fewer numbers of cells with shorter primary cilia (Figures S5G and S5H). Together, our results indicate that Src, YES, or FYN are not required for cilia formation and that ectopic p60 Src levels and/or activity during G1 inhibit ciliogenesis.

Our results suggested that MIM promotes ciliogenesis by inhibiting Src activation and that in the absence of *Src* MIM may not be required to maintain cilia. As predicted, MIM KD does not significantly reduce cilia in $SYF^{-/-}$ MEFs (Figures 5I and 5J), while the same degree of knockdown has a strong effect in wild-type cells (Figures 1B, 1D, and 4C). On the other hand,

(I and J) MIM KD in $SYF^{-/-}$ and $SYF^{-/-}$; *Src+* MEFs. (I) Western analysis for MIM, activated p-SRC Y416 and Actin. The numbers below the blots indicate relative protein levels in each lane. (J) Percentage of cilia. More than 350 cells were analyzed in three experiments.

(K and L) $SYF^{-/-}$ MEFs were transfected with the indicated DsRed CTTN or GFP SRC constructs and the effect of the corresponding proteins on primary cilia was compared to $SYF^{-/-}$ MEFs transfected with DsRed/GFP plasmids as well as to untransfected $SYF^{-/-}$; *Src+* MEFs. (K) Western analysis for the indicated proteins. Notes: GFP SRC proteins are higher MW than endogenous SRC and are not shown in the western blot; however, their expression and function is evident from induction of p-CTTN Y421. Also, while $SYF^{-/-}$ MEFs have plenty of endogenous CTTN, it is not normally phosphorylated. (L) Percentage of transfected (except in the case of $SYF^{-/-}$; *Src+*) cells with primary cilia. More than 300 cells were analyzed in three experiments. In all the figures error bars show SEM. Statistics: unpaired two-tailed t tests were done for experiments that were performed at least three times. Stars indicate statistically significant differences. *p < 0.05; **p < 0.01; ***p < 0.001.

(M) Model of how MIM promotes ciliogenesis by inhibiting Src activation and CTTN phosphorylation. Normally during G1/S the relative ratio of MIM to pSrc and pCTTN is high, which was shown in vitro to inhibit actin polymerization (Lin et al., 2005). We find that inhibition of actin polymerization promotes cilia maintenance and elongation. As the cell cycle progresses, a drop in the ratio of MIM to pSrc and pCTTN levels promotes increased F-actin polymerization, which inhibits ciliogenesis and promotes disassembly. In MIM KD cells activation of Src leads to upregulation of pCTTN, shifting the relative ratio of MIM to pCTTN to low (similar to what is seen normally during G2/M), which correlates with increased actin polymerization and inhibits ciliogenesis.

MIM KD in $SYF^{-/-}$; $Src+$ MEFs further increases the level of activating p-Src Y416 and further decreases the percentage of ciliated cells (Figures 5I and 5J). These results suggest that MIM promotes ciliogenesis by functioning upstream of Src and inhibiting Src activation during G1. Interestingly, the C-terminal MIM construct (amino acids 400–755) that localizes to the basal body and rescues primary cilia is phosphorylated by purified Src in vitro (Figure S5I), which suggested that MIM could inhibit Src through direct competition for the active site. However, GST-MIM does not inhibit CTTN phosphorylation by Src in vitro (Figure S5I), arguing that MIM-dependent inhibition of Src is likely mediated through its interactions with additional regulatory proteins.

Finally, to further test whether phosphorylated/activated CTTN is the causative inhibitor of ciliogenesis, we expressed RFP-tagged wild-type, nonphosphorylatable (YFM3) or phospho-mimetic (YEM3) CTTN mutants in $SYF^{-/-}$ MEFs and assessed primary cilia in transfected cells. As a positive control, we compared the effect of CTTN with that of GFP-tagged wild-type or constitutively active (Y527F) SRC. We find that wild-type or YFM3 CTTN has no effect on the cilia status of cells, while activated YEM3 CTTN significantly reduces ciliation (Figures 5K, 5L, and S5J). However, this effect is weaker than that of either wild-type or constitutively active Src (Figures 5K and 5L), which can often be detected colocalized with a disorganized array of acetylated microtubules at the site where the primary cilium would emerge (arrows in Figure S5J). Collectively, our results suggest that activated CTTN is sufficient to inhibit ciliogenesis and is a critical effector downstream of Src, although other Src substrates may play additional roles in ciliogenesis (Figure 5M).

MIM-Dependent Inhibition of Src and Cortactin Is Required for Dermal Shh Reception

Given MIM's function in promoting ciliogenesis and the critical role for primary cilia in Shh signal transduction (Huangfu and Anderson, 2005), we tested if MIM is required for Shh signaling. Toward this end, we measured endogenous target gene expression before and after stimulation with ShhN ligand and observed a dramatic decrease in activation of multiple Shh target genes upon MIM KD (Figures 6A and 6B). This phenotype is dose dependent and seen in multiple cell types and with several independent hairpins (Figures S6A–S6D and data not shown). The effect of MIM KD on primary cilia and Shh responsiveness was comparable to that seen with reduction in IFT88 levels and therefore consistent with the proposed effects of MIM on the primary cilium (Figures S6E and S6F).

Because of the antagonistic relationship between MIM and CTTN in ciliogenesis, we next examined their functional interaction in Shh signaling. While MIM KD alone inhibits Shh responsiveness, CTTN KD does not have a consistent significant effect (Figures 6C and 6D). In striking similarity to the cilia phenotype, Shh target gene induction is restored to control levels upon simultaneous depletion of MIM and CTTN (Figures 6C–6E). Taken together, these results indicate that MIM is required for Shh signal responsiveness and functions in part by antagonizing CTTN to allow primary cilia formation.

Previously we showed using gain-of-function approaches that MIM potentiates Shh signaling through interactions with Gli and Sufu (Callahan et al., 2004), which suggested a direct role for MIM in the pathway. To address a separate, cilia-independent role for endogenous MIM in regulating Shh signaling, we investigated the effect of MIM KD on Shh responsiveness in $SYF^{-/-}$ MEFs, where MIM does not affect ciliogenesis (Figures 5I and 5J). Strikingly, while cells lacking *Src, Yes*, and *Fyn* tyrosine kinases are robustly Shh responsive, overexpression of p60 *Src* abolishes their ability to induce Shh target genes (Figure 6F and data not shown). Surprisingly, MIM KD in $SYF^{-/-}$ MEFs no longer inhibits Shh responsiveness (Figure 6F and data not shown), suggesting that MIM is required for Shh signaling indirectly, through its role in ciliogenesis. Nevertheless, it is formally possible that MIM may regulate Gli trafficking to the cilium in a Src/CTTN-dependent manner. Consistent with this idea, we find that, while MIM does not alter total Gli1 and Gli2 protein levels, it does promote their accumulation at the basal body (Figures 6G and 6H).

Dermal MIM Is Required for Hair Follicle Regeneration

Recent studies have uncovered a key role for dermal primary cilia in regulating hair follicle morphogenesis (Lehman et al., 2009). Primary cilia are abundant in skin and hair follicles throughout both epithelial and mesenchymal compartments, with the majority of cilia observed at the base of hair follicles where highly proliferative matrix keratinocytes and dermal papilla cells reside (Figure 7A and data not shown). MIM is ubiquitously expressed in hair follicles with punctate cytoplasmic localization and strong enrichment at the basal body (Figures 7B and 7B′), similar to the pattern observed in cultured cells. Given MIM's function in ciliogenesis, we tested if dermal MIM is required in vivo for hair follicle reconstitution (Lichti et al., 2008). We confirmed that control dermal cells combined with wild-type keratinocytes efficiently regenerate new hair follicles that progress into late anagen (stage 4–6) (Muller-Rover et al., 2001) after 3 weeks (Figures 7C, 7F, and 7I). Moreover, the dermal papillae in control follicles display readily detectible primary cilia on almost every cell (Figures 7L and 7L′).

In contrast, dermal MIM KD with two different hairpins prevents hair follicle regeneration (Figures 7D–7K). The few follicles that form are less mature, between stage 2 and 4 of anagen (Figures 7J and 7K) but display markers of differentiation such as hair keratin AE13 (Figure S7A). Mutant follicles typically have abnormal morphology (Figure 7J) and small dermal papilla (Figure 7K). In rare cases when regular size dermal papillae are detected, they are largely devoid of primary cilia (Figures 7M and 7M′). Epithelial primary cilia, on the other hand, remain intact after dermal MIM KD (Figure S7B). The severe lack of hair combined with hair follicle arrest is strikingly similar to the phenotypes observed in dermal *Ift88* or *Kif3A* mutants and in *Shh* null mice (Chiang et al., 1999; Lehman et al., 2009; St-Jacques et al., 1998), suggesting that MIM maintains dermal primary cilia presumably to facilitate epithelial-mesenchymal Shh signaling during hair follicle regeneration.

DISCUSSION

We have shown that MIM promotes ciliogenesis by inhibiting Src kinase activation during G1. Decreased levels of MIM lead to upregulation of activated Src and subsequent
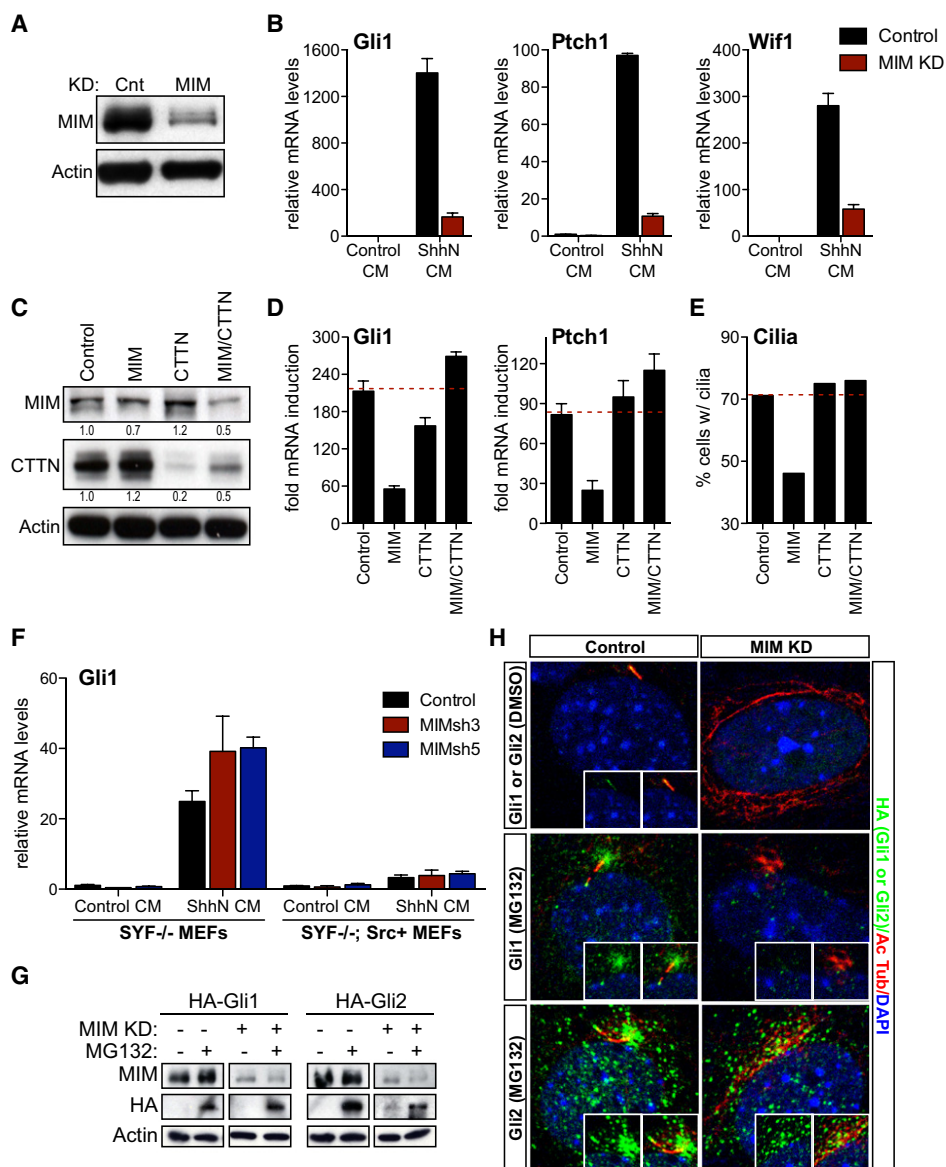
Figure 6. MIM Is Required for Dermal Shh Signal Responsiveness

(A and B) Following MIM KD, confluent cultures of primary mouse dermal cells were treated with control or ShhN conditioned media (CM). (A) Western analysis for MIM. (B) qRT-PCR results showing relative mRNA levels of the indicated genes.

(C–E) Following control, MIM, CTTN, or MIM/CTTN KD, confluent cultures of primary mouse dermal cells were treated with control or ShhN CM. (C) Western analysis for MIM, CTTN, and Actin. The numbers below indicate relative protein levels in each lane. (D) qRT-PCR results showing fold Gli1 and Ptch1 mRNA induction with ShhN normalized to control CM. (E) Percentage of cells with cilia in this experiment.

(F) Following MIM KD with two separate hairpins, confluent cultures of $SYF^{-/-}$ and $SYF^{-/-}; Src+$ MEFs were treated with control or ShhN CM. qRT-PCR results of relative Gli1 mRNA levels are shown. Similar results were obtained for Ptch1 (not shown).

(G and H) Control or MIM KD primary dermal cells were transduced with retroviral constructs expressing HA-hGli1 or HA-mGli2 and treated with DMSO or MG132 for 4 hr. (G) Western analysis for MIM, HA-Gli1, HA-Gli2, and Actin. (H) Representative IF images with antibody to acetylated α-tubulin (red), HA-tag (green), and DNA (blue). Where applicable, error bars show SD based on three technical replicates.

hyperphosphorylation of multiple actin-associated Src substrates including CTTN, which promotes increased F-actin branching and polymerization. Importantly, either inhibition of the Src catalytic domain or removal of CTTN is sufficient to restore ciliogenesis in the absence of MIM, suggesting that MIM regulates an intricate balance of actin regulatory factors that affect cilia dynamics, but is not uniquely required for ciliogenesis. Among the critical functional consequences of this deregulation in mesenchymal cells are failure to respond to Shh signaling and inability to induce hair growth. Collectively, our data reveal a mechanism that coordinates ciliogenesis with cell cycle progression and provide a strong connection between actin cytoskeletal regulators, ciliogenesis, and Shh signaling during tissue regeneration.
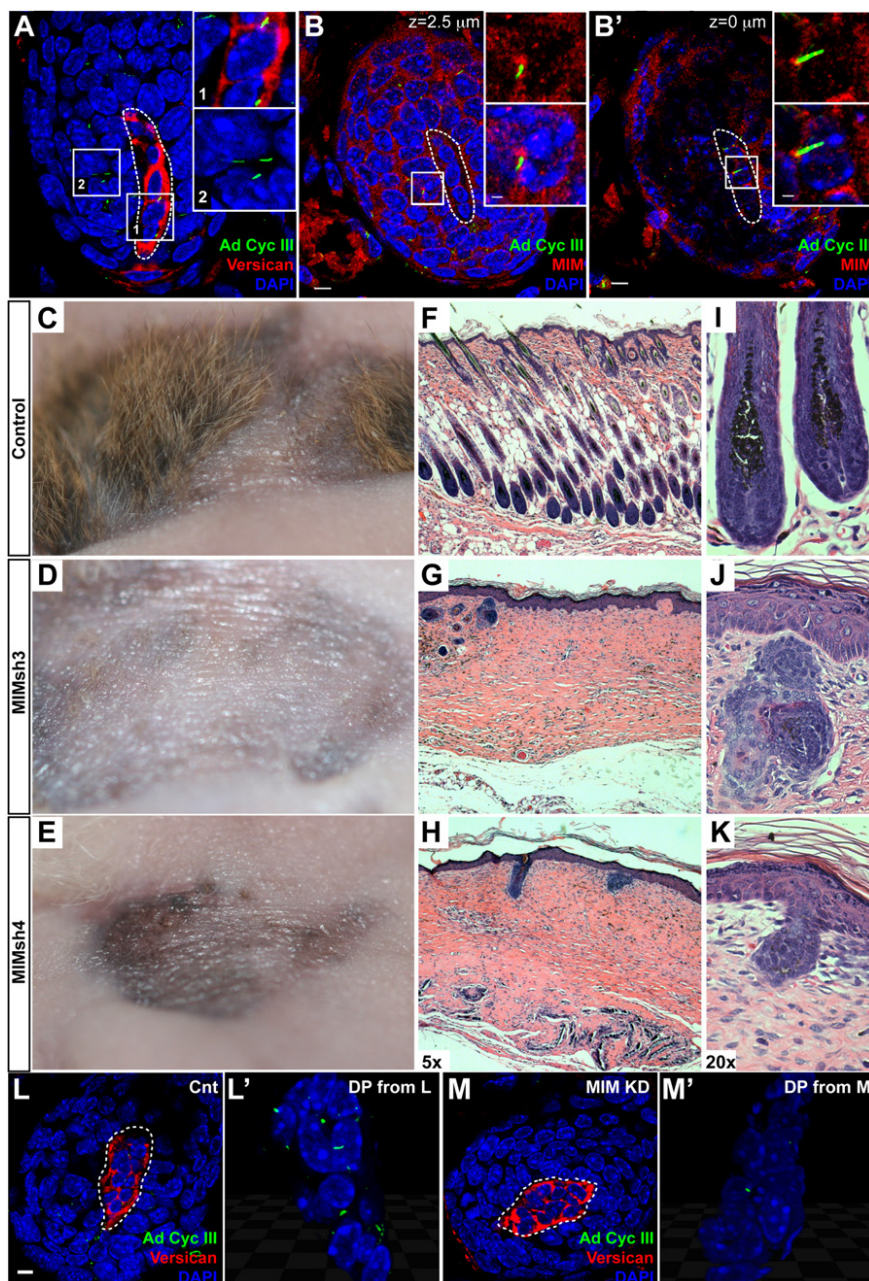
Figure 7. Dermal MIM Is Required for Hair Follicle Regeneration

(A) Longitudinal section of an anagen hair follicle showing the distal portion or base of the follicle. IF with antibodies to Adenyl Cyclase III (green) to mark the primary cilia, Versican (red) to mark the dermal papilla (DP, outlined by the dotted white line), and DNA (blue). Boxes 1 and 2 in the main image are shown at higher magnification to the right. Box 1 shows primary cilia in DP cells and Box 2 shows primary cilia in nearby keratinocytes.

(B) Cross section of an anagen hair follicle at the base. IF with antibodies to Adenyl Cyclase III (green), MIM (red), and DNA (blue). The DP is outlined by the dotted white line. Scale bar represents 5 μm in the main images and 1 μm in the insets.

(B and B') Two different confocal z-planes showing that MIM immunoreactivity at the ciliary base is enriched in keratinocytes (B) and in DP cells (B').

(C–E) Photographs of representative control and MIM KD grafts. A total of two to four grafts were performed in each case.

(F–K) Representative H&E sections from control and MIM KD grafts. Original magnification was 5× (F–H) and 20× (I–K).

(L and M) IF of a representative control (L) and MIM KD (M) hair follicles with antibodies against Adenyl Cyclase III (green), Versican (red), and DNA (blue). DP is outlined by the dotted white line. Scale bar represents 5 μm. (L' and M') 3D projection of the DP from the control (L) or MIM KD (M) hair follicle.

of the hair follicle phenotype and underscores the importance for dermal primary cilia in hair follicle development. Thus, our results support a key role for MIM in dermal cilia regulation and Shh signaling during de novo hair formation and demonstrate the utility of the hair regeneration system for rapid screening, identification, and analysis of in vivo, cell type-specific regulators of hair formation.

MIM Knockdown Reveals an Inhibitory Role for Src Kinase during Ciliogenesis

Our data point to a model whereby MIM promotes ciliogenesis by antagonizing Src activity during G1. MIM's inhibitory effect on Src is highlighted by the fact that multiple Src substrates, including other kinases, scaffolding proteins, and actin cytoskeleton regulators known to affect cell proliferation, adhesion and migration, become hyperphosphorylated upon MIM KD. This finding provides a potential basis for the frequent alteration of MIM levels in metastatic cancers, as Src is a well-known oncogene and the hyperphosphorylated substrates that we detect are all associated with decreased cell adhesion and increased cell motility (Mitra and Schlaepfer, 2006). However, with respect to Src-dependent cilia disassembly, the Src substrate CTTN appears to be a key downstream effector, since CTTN KD impairs cilia resorption and removal of CTTN is sufficient to restore cilia in MIM KD cells.

MIM Is Required for Primary Cilia Formation, Shh Signaling, and Hair Follicle Regeneration

Much like the developing node and the limbs, the hair follicles rely on primary cilia to transduce signals from Shh (Huangfu and Anderson, 2005; Huangfu et al., 2003; Lehman et al., 2009) and other morphogens. Reduction in MIM levels in the dermal compartment leads to severe lack of hair and immature follicles that appear arrested at stage 2–4 of anagen, similar to the phenotypes observed upon dermal cilia ablation through conditional deletion of *Ift88* or *Kif3A* (Lehman et al., 2009) or in *Shh* mutant skin (Chiang et al., 1999; St-Jacques et al., 1998). The fact that MIM KD disrupts primary cilia in the regenerated dermal papillae provides additional evidence that the cilia defect forms the basis

Several independent lines of evidence support our model that ectopic Src kinase activity during G1 inhibits ciliogenesis. First, the cilia defect in MIM KD cells can be rescued by several small molecule inhibitors of the SFK family (Figures 5D–5F). Second, overexpression of just p60 Src in $SYF^{-/-}$ MEFs potently inhibits ciliogenesis and completely abolishes any Shh responsiveness, despite the fact that most of the cells are in G1/G0 (Figures 5G, 5H, 6F, and S5D–S5F). Third, transient expression of a constitutively active Src Y527F mutant reveals basal body localization and inhibits ciliogenesis in $SYF^{-/-}$ MEFs and primary dermal cells in a cell-autonomous manner (Figures 5L, S5H, and S5J). Finally, fourth: transiently expressed kinase dead Src K295R mutant functions as a dominant-negative with respect to p-CTTN and induces more and longer cilia in dermal cells (Figure S5H). These data point to the powerful inhibitory actions of Src kinase and the critical need to restrain its activity during G1.

MIM and Cortactin Antagonism Act as a Switch to Regulate Ciliogenesis

Emerging data support the idea that the basal body coordinates ciliogenesis with the cell cycle. This regulation is likely based on a dynamic cell-cycle-dependent equilibrium between factors that promote cilia formation after cytokinesis and factors that promote cilia disassembly prior to mitosis. MIM and CTTN appear to be two such factors, with MIM promoting cilia formation and Src-activated p-CTTN promoting cilia disassembly. Based on our results, we propose a model whereby MIM antagonism of p-CTTN serves as a switch to regulate the timing of ciliogenesis and coordinate it with the cell cycle (Figure 5M). Thus during G1/S, when the relative ratio of MIM to p-CTTN is high, cilia are maintained. As the cell cycle progresses toward G2/M, activation of Src leads to increased p-CTTN levels, shifting the ratio of MIM to p-CTTN to low and inducing cilia disassembly. When MIM is depleted, activation of Src leads to upregulation of p-CTTN during G1, artificially shifting the ratio of MIM to p-CTTN to resemble what it normally is during G2/M. Interestingly MIM-depleted cells display ectopic p-Src and p-CTTN in the cytosol and at the basal body, suggesting that Src and CTTN functions outside the basal body may also contribute to cilia maintenance. This is supported by the finding that inhibition of Src or depletion of CTTN restores cilia in MIM KD cells and underscores the critical relationship between MIM and Src activity.

Our findings combined with multiple lines of published data suggest that MIM and CTTN antagonism affects ciliogenesis by regulating the actin cytoskeleton. First of all, the antagonism between MIM and CTTN appears to be conserved in evolution and "recycled" for multiple actin-dependent cellular processes including *Drosophila* border cells migration and clathrin-mediated endocytosis (Quinones et al., 2010). Moreover, high levels of MIM relative to CTTN were shown in vitro to inhibit CTTN mediated actin polymerization (Lin et al., 2005). On the other hand, phosphorylation by Src is known to increase CTTN affinity and nucleating activity for F-actin (Ammer and Weed, 2008; Lua and Low, 2005; Kruchten et al., 2008). Moreover, recent studies in NIH 3T3 and HeLa cells found that p-CTTN Y466/Y421 is enriched at the centrosomes during G2/M and mediates actin-dependent centrosome separation (Wang et al., 2008). Consistent with all of these data, we see increased levels and disorga-

nized F-actin staining in MIM KD cells that lack cilia and vice versa, reduced F-actin staining in CTTN KD cells that fail to disassemble their cilia. In addition, disruption of F-actin with polymerization inhibitors causes cilia elongation and prevents cilia disassembly. Thus, while F-actin may be required for initial basal body motility and membrane docking (Pan et al., 2007; Vladar and Axelrod, 2008), our data suggest that F-actin needs to be cleared locally during G1 to allow cilia elongation and maintenance and then reformed later in the cell cycle to promote cilia disassembly. Interestingly, a recent screen for genes involved in ciliogenesis identified several regulators of actin dynamics and vesicle trafficking (Kim et al., 2010), and actin clearing by the centrosome has been shown to be required in other directed membrane events such as exocytosis of lytic granules (Stinchcombe et al., 2006). Moreover, Septin2, known to play a role in actin dynamics, appears to play a role in maintaining the ciliary protein diffusion barrier and proper signaling (Hu et al., 2010). Therefore, actin regulatory proteins localized at the basal body such as MIM and CTTN could provide a general mechanism for regulating directional plasma membrane remodeling and proper cilium-dependent signaling.

EXPERIMENTAL PROCEDURES

Lentiviral Knockdown

Hairpins were designed using PSicoOligomaker 1.5 software (http://web.mit.edu/jacks-lab/protocols/pSico.html) and cloned into pSicoR-puro lentiviral vector (Ventura et al., 2004). For MIM KD, the following target sequences were used: GGAAGAGATTTCCATGTTA (sh3), GTACAACTATGTCCAGAAA (sh4), GCAAGGCACTCATCGAAGA (sh5). For CTTN KD, the following target sequence was used: GCACAGGGTTCACACTACA (sh1). IFT88 hairpin expressed from pSicoR-puro vector was a kind gift from T. Stearns (Vladar and Stearns, 2007). All assays were performed between 4 and 10 days after initial lentivral infection, upon confirmation of successful protein knockdown by western blot or immunofluorescence.

Cell Culture

Early passage primary mouse dermal cells were grown in Amnio MAX medium with supplement (Invitrogen). All cell lines (C3H10T1/2 [referred to as 10T1/2], MEF, NIH 3T3, 293T) were cultured using standard conditions. $SYF^{-/-}$ and $SYF^{-/-}; Src+$ MEFs were obtained from ATCC.

Cilia Assembly and Disassembly Assays

To examine primary cilia, equal numbers of control or experimental cells were plated at confluence (typically ~10^5 cells/cm^2) onto four-well glass chamber slides in regular culture medium. Prior to fixation and staining cells were typically serum starved for 24 hr. For disassembly assays, serum-starved cells were incubated with DMEM containing 10% FBS for 2–6 hr as indicated. To estimate percentage of ciliated cells in each experiment, several hundred cells from representative fields were scored under the microscope for presence of primary cilia.

Inhibitors

Src inhibitor I, SU6656, and MG132 were from Calbiochem; DMSO, cytochalasin B, cytochalasin D, nocodazole, sodium orthovanadate, and sodium fluoride were from Sigma; complete protease inhibitor mix was from Roche. For the Src inhibition assays, serum-starved cells were incubated with drugs used at 3× IC_{50} prior to lysis or fixation: Src inhibitor I (130 nM) for 2 hr; SU6656 (840 nM) for 6 hr. To disrupt F-actin, cytochalasin B and D were used at 5 mM.

Immunocytochemistry

To stain primary cilia, cells were fixed with 4% paraformaldehyde at room temperature for 15 min. To stain centriolar proteins, cells were fixed with

cold methanol on ice for 10 min. Blocking was done with 1% normal horse serum and 0.1% Triton X-100 in PBS for 30 min at room temperature. Antibodies were washed away with PBS, and secondary detection was performed with Alexa-conjugated fluorophores (1:500). Nuclei were stained with Hoechst 33258 diluted 1:10,000 in PBS. F-actin was visualized with phalloidin AF633 (Invitrogen, 1:100).

Immunoprecipitations
Cells were lysed in using 20 mM HEPES (pH 7.9), 150 mM NaCl, 1% NP-40, 0.5 mM Na_3VO_4, 20 mM NaF, and protease inhibitor cocktail. Lysates were incubated with primary antibodies for 2 hr or overnight at 4°C. Immunocomplexes were collected using agarose beads, washed four times in lysis buffer, and resolved by SDS-PAGE.

Cell Synchronization
Primary dermal cells were synchronized by serum starvation for 48 hr and released back into cycle by addition of serum-containing medium. Cell cycle progression was monitored every 4 hr for the following 44 hr by cell counting, visual inspection, and expression of known cell cycle regulators.

Primary Antibodies
A complete list of antibodies with applications and dilutions is provided in the Supplemental Information.

Centrosome Purification
Centrosomes were purified from C3H10T1/2 cells as previously described (Meigs and Kaplan, 2008).

Isolation of Primary Dermal and Epidermal Cells
To isolate primary dermal cells and keratinocytes, skin was dissected from 1- to 3-day-old pups and incubated in 50% dispase solution overnight at 4°C. To dissociate tissues into single cells, pieces of dermis were incubated in collagenase solution containing antibiotics at 37°C for 40–60 min, while pieces of epidermis were incubated in 0.05% trypsin at 37°C for 15 min. Cell suspensions were then neutralized with FBS, passed through a 70 μm strainer, and spun down.

Hair Regeneration Genetic Assay
We adopted the hair regeneration assay originally developed by Lichti et al. (2008) for use with lentiviral-based shRNA-mediated gene knockdown. In brief, 1- to 3-day-old mice from crosses between CD1 females and C57BL/6 males were used for isolation of epidermal and dermal cells (see Supplemental Experimental Procedures) and grafted onto 8- to 12-week-old nude female mice. Isolated dermal cells were seeded onto 10 cm plates and infected with pSicoR viruses the following day. Twenty-four hours post-infection, 10×10^6 dermal cells were mixed with freshly isolated epidermal cells at a 1:1 ratio and seeded onto each graft. The hair phenotype was analyzed 3 weeks after cell application.

SUPPLEMENTAL INFORMATION

Supplemental Information includes Supplemental Experimental Procedures and seven figures and can be found with this article online at doi:10.1016/j.devcel.2010.07.009.

REFERENCES

Adams, M., Smith, U.M., Logan, C.V., and Johnson, C.A. (2008). Recent advances in the molecular pathology, cell biology and genetics of ciliopathies. J. Med. Genet. *45*, 257–267.

Ammer, A.G., and Weed, S.A. (2008). Cortactin branches out: roles in regulating protrusive actin dynamics. Cell Motil. Cytoskeleton *65*, 687–707.

Bompard, G., Sharp, S.J., Freiss, G., and Machesky, L.M. (2005). Involvement of Rac in actin cytoskeleton rearrangements induced by MIM-B. J. Cell Sci. *118*, 5393–5403.

Callahan, C.A., Ofstad, T., Horng, L., Wang, J.K., Zhen, H.H., Coulombe, P.A., and Oro, A.E. (2004). MIM/BEG4, a Sonic hedgehog-responsive gene that potentiates Gli-dependent transcription. Genes Dev. *18*, 2724–2729.

Caspary, T., Larkins, C.E., and Anderson, K.V. (2007). The graded response to Sonic Hedgehog depends on cilia architecture. Dev. Cell *12*, 767–778.

Chari, N.S., and McDonnell, T.J. (2007). The sonic hedgehog signaling network in development and neoplasia. Adv. Anat. Pathol. *14*, 344–352.

Chiang, C., Swan, R.Z., Grachtchouk, M., Bolinger, M., Litingtung, Y., Robertson, E.K., Cooper, M.K., Gaffield, W., Westphal, H., Beachy, P.A., et al. (1999). Essential role for Sonic hedgehog during hair follicle morphogenesis. Dev. Biol. *205*, 1–9.

Davenport, J.R., and Yoder, B.K. (2005). An incredible decade for the primary cilium: a look at a once-forgotten organelle. Am. J. Physiol. Renal Physiol. *289*, F1159–F1169.

Dawe, H.R., Farr, H., and Gull, K. (2007). Centriole/basal body morphogenesis and migration during ciliogenesis in animal cells. J. Cell Sci. *120*, 7–15.

Fliegauf, M., Benzing, T., and Omran, H. (2007). When cilia go bad: cilia defects and ciliopathies. Nat. Rev. Mol. Cell Biol. *8*, 880–893.

Graser, S., Stierhof, Y.D., Lavoie, S.B., Gassner, O.S., Lamia, S., Le Clech, M., and Nigg, E.A. (2007). Cep164, a novel centriole appendage protein required for primary cilium formation. J. Cell Biol. *179*, 321–330.

Gonzalez-Quevedo, R., Shoffer, M., Horng, L., and Oro, A.E. (2005). Receptor tyrosine phosphatase-dependent cytoskeletal remodeling by the hedgehog-responsive gene MIM/BEG4. J. Cell Biol. *168*, 453–463.

Haggarty, S.J., Koeller, K.M., Wong, J.C., Grozinger, C.M., and Schreiber, S.L. (2003). Domain-selective small-molecule inhibitor of histone deacetylatse 6 (HDAC6)-mediated tubulin deacetylation. Proc. Natl. Acad. Sci. USA *100*, 4389–4394.

Houde, C., Dickinson, R.J., Houtzager, V.M., Cullum, R., Montpetit, R., Metzler, M., Simpson, E.M., Roy, S., Hayden, M.R., Hoodless, P.A., et al. (2006). Hippi is essential for node cilia assembly and Sonic hedgehog signaling. Dev. Biol. *300*, 523–533.

Hu, Q., Milenkovic, L., Jin, H., Scott, M.P., Nachury, M.V., Spiliotis, E.T., and Nelson, W.J. (2010). A Septin Diffusion Barrier at the base of the primary cilium maintains ciliary membrane protein diffusion. Science, in press. Published online June 17, 2010. 10.1126/science.1191054.

Huangfu, D., and Anderson, K.V. (2005). Cilia and Hedgehog responsiveness in the mouse. Proc. Natl. Acad. Sci. USA *102*, 11325–11330.

Huangfu, D., Liu, A., Rakeman, A.S., Murcia, N.S., Niswander, L., and Anderson, K.V. (2003). Hedgehog signalling in the mouse requires intraflagellar transport proteins. Nature *426*, 83–87.

Kaplan, D.D., Meigs, T.E., Kelly, P., and Casey, P.J. (2004). Identification of a role for beta-catenin in the establishment of a bipolar mitotic spindle. J. Biol. Chem. *279*, 10829–10832.

Karlsson, L., Bondjers, C., and Betsholtz, C. (1999). Roles for PDGF-A and sonic hedgehog in development of mesenchymal components of the hair follicle. Development *126*, 2611–2621.

Kim, J., Lee, J.E., Heynen-Genel, S., Suyama, E., Ono, K., Lee, K., Ideker, T., Aza-Blanc, P., and Gleeson, J.G. (2010). Functional genomic screen for modulators of ciliogenesis and cilium length. Nature *464*, 1048–1051.

Kruchten, A.E., Krueger, E.W., Wang, Y., and McNiven, M.A. (2008). Distinct phospho-forms of cortactin differentially regulate actin polymerization and focal adhesions. Am. J. Physiol. Cell Physiol. *295*, C1113–C1122.

Lange, B.M., and Gull, K. (1995). A molecular marker for centriole maturation in the mammalian cell cycle. J. Cell Biol. *130*, 919–927.

Lehman, J.M., Laag, E., Michaud, E.J., and Yoder, B.K. (2009). An essential role for dermal primary cilia in hair follicle morphogenesis. J. Invest. Dermatol. *129*, 438–448.

Lichti, U., Anders, J., and Yuspa, S.H. (2008). Isolation and short-term culture of primary keratinocytes, hair follicle populations and dermal cells from newborn mice and keratinocytes from adult mice for in vitro analysis and for grafting to immunodeficient mice. Nat. Protoc. *3*, 799–810.

Lin, J., Liu, J., Wang, Y., Zhu, J., Zhou, K., Smith, N., and Zhan, X. (2005). Differential regulation of cortactin and N-WASP-mediated actin polymerization by missing in metastasis (MIM) protein. Oncogene *24*, 2059–2066.

Lua, B.L., and Low, B.C. (2005). Cortactin phosphorylation as a switch for actin cytoskeletal network and cell dynamics control. FEBS Lett. *579*, 577–585.

Machesky, L.M., and Johnston, S.A. (2007). MIM: a multifunctional scaffold protein. J. Mol. Med. *85*, 569–576.

Marshall, W.F. (2008). Basal bodies platforms for building cilia. Curr. Top. Dev. Biol. *85*, 1–22.

Mattila, P.K., Pykalainen, A., Saarikangas, J., Paavilainen, V.O., Vihinen, H., Jokitalo, E., and Lappalainen, P. (2007). Missing-in-metastasis and IRSp53 deform PI(4,5)P2-rich membranes by an inverse BAR domain-like mechanism. J. Cell Biol. *176*, 953–964.

Mattila, P.K., Salminen, M., Yamashiro, T., and Lappalainen, P. (2003). Mouse MIM, a tissue-specific regulator of cytoskeletal dynamics, interacts with ATP-actin monomers through its C-terminal WH2 domain. J. Biol. Chem. *278*, 8452–8459.

Meigs, T.E., and Kaplan, D.D. (2008). Isolation of centrosomes from cultured mammalian cells. Cold Spring Harb. Protoc. 10.1101/pdb.prot5039.

Mitra, S.K., and Schlaepfer, D.D. (2006). Integrin-regulated FAK-Src signaling in normal and cancer cells. Curr. Opin. Cell Biol. *18*, 516–523.

Mogensen, M.M., Malik, A., Piel, M., Bouckson-Castaing, V., and Bornens, M. (2000). Microtubule minus-end anchorage at centrosomal and non-centrosomal sites: the role of ninein. J. Cell Sci. *113*, 3013–3023.

Muller-Rover, S., Handjiski, B., van der Veen, C., Eichmuller, S., Foitzik, K., McKay, I.A., Stenn, K.S., and Paus, R. (2001). A comprehensive guide for the accurate classification of murine hair follicles in distinct hair cycle stages. J. Invest. Dermatol. *117*, 3–15.

Nachury, M.V., Loktev, A.V., Zhang, Q., Westlake, C.J., Peranen, J., Merdes, A., Slusarski, D.C., Scheller, R.H., Bazan, J.F., Sheffield, V.C., et al. (2007). A core complex of BBS proteins cooperates with the GTPase Rab8 to promote ciliary membrane biogenesis. Cell *129*, 1201–1213.

Norman, R.X., Ko, H.W., Huang, V., Eun, C.M., Abler, L.L., Zhang, Z., Sun, X., and Eggenschwiler, J.T. (2009). Tubby-like protein 3 (TULP3) regulates patterning in the mouse embryo through inhibition of Hedgehog signaling. Hum. Mol. Genet. *18*, 1740–1754.

Pan, J., You, Y., Huang, T., and Brody, S.L. (2007). RhoA-mediated apical actin enrichment is required for ciliogenesis and promoted by Foxj1. J. Cell Sci. *120*, 1868–1876.

Pearson, C.G., Culver, B.P., and Winey, M. (2007). Centrioles want to move out and make cilia. Dev. Cell *13*, 319–321.

Pugacheva, E.N., Jablonski, S.A., Hartman, T.R., Henske, E.P., and Golemis, E.A. (2007). HEF1-dependent Aurora A activation induces disassembly of the primary cilium. Cell *129*, 1351–1363.

Quinones, G.A., Jin, L., and Oro, A.E. (2010). I-BAR protein antagonism of endocytosis mediates directional sensing during guided cell migration. J. Cell Biol. *189*, 353–367.

Ruiz-Perez, V.L., Blair, H.J., Rodriguez-Andres, M.E., Blanco, M.J., Wilson, A., Liu, Y.N., Miles, C., Peters, H., and Goodship, J.A. (2007). Evc is a positive mediator of Ihh-regulated bone growth that localises at the base of chondrocyte cilia. Development *134*, 2903–2912.

Schneider, M.R., Schmidt-Ullrich, R., and Paus, R. (2009). The hair follicle as a dynamic miniorgan. Curr. Biol. *19*, R132–R142.

St-Jacques, B., Dassule, H.R., Karavanova, I., Botchkarev, V.A., Li, J., Danielian, P.S., McMahon, J.A., Lewis, P.M., Paus, R., and McMahon, A.P. (1998). Sonic hedgehog signaling is essential for hair development. Curr. Biol. *8*, 1058–1068.

Stinchcombe, J.C., Majorovits, E., Bossi, G., Fuller, S., and Griffiths, G.M. (2006). Centrosome polarization delivers secretory granules to the immunological synapse. Nature *443*, 462–465.

Ventura, A., Meissner, A., Dillon, C.P., McManus, M., Sharp, P.A., Van Parijs, L., Jaenisch, R., and Jacks, T. (2004). Cre-lox-regulated conditional RNA interference from transgenes. Proc. Natl. Acad. Sci. USA *101*, 10380–10385.

Vladar, E.K., and Axelrod, J.D. (2008). Dishevelled links basal body docking and orientation in ciliated epithelial cells. Trends Cell Biol. *18*, 517–520.

Vladar, E.K., and Stearns, T. (2007). Molecular characterization of centriole assembly in ciliated epithelial cells. J. Cell Biol. *178*, 31–42.

Wang, W., Chen, L., Ding, Y., Jin, J., and Liao, K. (2008). Centrosome separation driven by actin-microfilaments during mitosis is mediated by centrosome-associated tyrosine-phosphorylated cortactin. J. Cell Sci. *121*, 1334–1343.

Yamagishi, A., Masuda, M., Ohki, T., Onishi, H., and Mochizuki, N. (2004b). A novel actin-bundling/filopodium-forming domain conserved in insulin receptor tyrosine kinase substrate p53 and missing in metastasis protein. J. Biol. Chem. *279*, 14929–14936.

Yoshida, M., Kijima, M., Akita, M., and Beppu, T. (1990). Potent and specific inhibition of mammalian histone deacetylase both in vivo and in vitro by trichostatis A. J. Biol. Chem. *265*, 17174–17179.

Zhang, X., Yuan, Z., Zhang, Y., Yong, S., Salas-Burgos, A., Koomen, J., Olashaw, N., Parsons, J.T., Yang, X.J., Dent, S.R., et al. (2007). HDAC6 modulates cell motility by altering the acetylation level of cortactin. Mol. Cell *27*, 197–213.

Zhang, Y., Kwon, S., Yamaguchi, T., Cubizolles, F., Rousseaux, S., Kneissel, M., Cao, C., Li, N., Cheng, H., Chua, K., et al. (2008). Mice Lacking Histone Deacetylase 6 have hyperacetylated tubulin but are viable and develop normally. Mol. Cell. Biol. *28*, 1688–1701.